Clinical Cancer Research

Efficacy and Biological Activity of Imatinib in Metastatic Dermatofibrosarcoma Protuberans (DFSP)

Silvia Stacchiotti[1], Maria A. Pantaleo[2], Tiziana Negri[3], Annalisa Astolfi[4], Marcella Tazzari[5], Gian Paolo Dagrada[3], Milena Urbini[4], Valentina Indio[4], Roberta Maestro[6], Alessandro Gronchi[7], Marco Fiore[7], Angelo P. Dei Tos[8], Elena Conca[3], Elena Palassini[1], Bruno Vincenzi[9], Federica Grosso[10], Silvana Pilotti[3], Chiara Castelli[5], and Paolo G. Casali[1]

Abstract

Purpose: To report on imatinib mesylate (IM) in patients with metastatic dermatofibrosarcoma protuberans (DFSP)/fibrosarcomatous (FS)-DFSP and on the impact of the treatment on tumor biology.

Experimental design: Ten consecutive patients treated with IM from 2007 to 2015 for a metastatic relapse from DFSP/FS-DFSP were identified. FISH analysis for *COL1A1-PDGFB* was performed. Two IM-treated and 4 naïve FS-DFSP were transcriptionally profiled by RNAseq on HiScanSQ platform. Differential gene expression was analyzed with edgeR (Bioconductor), followed by hierarchical clustering and Principal Component Analysis.

Results: All cases featured fibrosarcomatous in the metastasis and retained the *COL1A1-PDGFB*. Best RECIST response was: 8 partial response, 1 stable disease, and 1 progressive disease. Median progression-free survival was 11 months. Five patients received surgery after IM and all relapsed. IM was restored in 4 patients with a new response. After IM, the most upregulated genes included those encoding for immunoglobulins and those affecting functions and differentiation of endothelial cells. Pathway enrichment analysis revealed upregulation in genes involved in antigen processing and presentation, natural killer–mediated cytotoxicity, and drug and xenobiotics metabolism. Conversely, a significant down-regulation of kinase signaling pathways was detected.

Conclusions: All metastatic cases were fibrosarcomatous. Most patients responded to IM, but PFS was shorter than reported in published series which included both DFSP and FS-DFSP. All patients operated after IM had a relapse, suggesting that IM cannot eradicate metastatic cases and that the role of surgery is limited. Transcriptional profile of naïve and posttreatment samples pointed the contribution of immune infiltrates in sustaining the response to IM. *Clin Cancer Res; 22(4); 837–46. ©2015 AACR.*

Introduction

Dermatofibrosarcoma protuberans (DFSP) is a rare sarcoma (1), arising from the skin and marked by rearrangement of chromosomes 17 and 22, which results in the *COL1A1–PDGFB* fusion gene (2). This chimera is responsible for constitutive activation of Platelet Derived Growth Factor Receptor Beta (PDGFRB; ref. 3), by mean of an autocrine-paracrine loop.

DFSP is characterized by an indolent and locally invasive growth, with a very low metastatic potential that is usually related to the presence of a more aggressive, fibrosarcomatous (FS) component (1, 4–6). Standard treatment consists of wide surgical excision, by which a high cure rate is achieved (4). FS aspects are detected in 5% to 15% of DFSP (1, 4–6), and may be present in the primary tumor or may occur at the time of relapse. FS transformation is related to an increased risk of metastases, in the range of 10% to 15% (5, 6), that can be located to unusual anatomic sites as pancreas (7) and brain (5). Metastases in completely resected DFSP/FS-DFSP are an extremely rare event, which, on the basis of available evidence, might be estimated to be less than 0.05 new cases per 1,000,000 each year (5, 8). Moreover, diagnosis can be really challenging in metastatic cases, with FS transformation occurring over time and sometimes loss of a classic DFSP featured component.

Imatinib mesylate (IM) is approved for treatment of advanced DFSP, where its impressive activity has been related to the inhibition of PDGFRB (9, 10). In contrast, the role of IM in the metastatic setting is not clarified. Both the prospective and the retrospective studies reported so far analyzed locally advanced and metastatic patients together, and the efficacy of IM treatment

[1]Adult Mesenchymal Tumour and Rare Cancer Medical Oncology Unit, Cancer Medicine Department, Fondazione IRCCS Istituto Nazionale Tumori, Milan, Italy. [2]Dipartimento di Medicina Sperimentale, Specialistica e Diagnostica, Università di Bologna, Bologna, Italy. [3]Laboratory of Experimental Molecular Pathology, Department of Diagnostic Pathology and Laboratory, Fondazione IRCCS Istituto Nazionale Tumori, Milan, Italy. [4]Centro Interdipartimentale di Ricerche sul Cancro G. Prodi, Università di Bologna, Bologna, Italy. [5]Unit of Immunotherapy of Human Tumors, Fondazione IRCCS Istituto Nazionale Tumori, Milan, Italy. [6]Unit of Experimental Oncology 1, CRO Aviano National Cancer Institute, Aviano, Italy. [7]Melanoma and Sarcoma Unit, Department of Surgery, Fondazione IRCCS Istituto Nazionale Tumori, Milan, Italy. [8]Department of Anatomic Pathology, General Hospital of Treviso, Treviso, Italy. [9]Department Medical Oncology Campus Biomedico, Roma, Italy. [10]Oncology, SS Antonio e Biagio General Hospital, Alessandria, Italy.

Note: Supplementary data for this article are available at Clinical Cancer Research Online (http://clincancerres.aacrjournals.org/).

Prior presentation: The abstract (10553) was presented at the 2015 ASCO Annual Meeting in Chicago.

Corresponding Author: S. Stacchiotti, Fondazione IRCCS Istituto Nazionale dei Tumori, via Venezian 1, 20133 Milan, Italy. Phone: +39-0223902182; Fax: +39-0223902804; E-mail: silvia.stacchiotti@istitutotumori.mi.it

doi: 10.1158/1078-0432.CCR-15-1243

Translational Relevance

This article, focused on metastatic dermatofibrosarcoma protuberans (DFSP) treated with imatinib, highlights that, besides inhibiting tumoral PDGFRB, imatinib also affects tumor microenvironment, and suggests that the elicitation of an innate and adaptive immune response may be crucial in sustaining the response to the treatment. We confirm that imatinib is active in most cases but fails to eradicate the tumor, even after surgical excision of responsive residual disease. Thus, imatinib rechallenge after surgery may be a reasonable option. All our metastatic patients had aspects of fibrosarcomatous evolution.

was not investigated specifically in FS-DFSP (11–15). We already reported on 4 patients with advanced, translocated FS-DFSP (3 metastatic, one locally advanced) who received IM (5).

If on one side the clinical response to IM of FS-DFSP is still unclear, on the other side, the biology of DFSP undergoing FS evolution has been only marginally addressed (9, 16). In addition, little is known about gene expression profile of FS-DFSP and how IM treatment affects the gene expression profile of these lesions.

To shed light on these issues, we analyzed a retrospective series of 10 patients with metastatic DFSP/FS-DFSP, molecularly confirmed by the presence of *COL1A1–PDGFB* fusion gene, treated with IM at our institution and within the Italian Rare Cancer Network, from 2007 to 2015. Three of these patients were among the 4 previously reported (5). We describe their clinical behavior and we report on the gene expression profile (GEP) analysis performed in few naïve and IM-pretreated FS-DFSP tumor samples.

Materials and Methods

We retrospectively reviewed all consecutive adult patients treated with IM for metastatic relapse from DFSP or FS-DFSP at Fondazione IRCCS Istituto Nazionale dei Tumori, Milan, Italy (INT), and within the Italian Rare Cancer Network (IRCN) from 2007 to 2014. All cases treated with IM for local regional disease in the absence of metastatic lesions were excluded. Clinical data were extracted from the institutional and the Rare Cancer Network databases of all adult patients with soft tissue and bone sarcomas. The analysis was approved by the Institutional Ethics Committee.

Pathology

All cases were reviewed and reclassified applying updated criteria (17, 18). In all cases, the metastatic disease was assessed histologically and diagnosis confirmed. The primary lesion and metastases were compared in all patients, retrieving the tissue of the primary tumor that in 7 cases was resected and sampled elsewhere, whereas in 3 patients, the primary was operated at INT (Table 1). FS change was defined by the appearance in a classical storiform DFSP of at least 5% of high cellular area made up of spindle cells arranged in an herringbone pattern with a mitotic index >7/10 high power field (17); necrosis, pleomorphic features, myofibroblastic differentiation were also recorded and considered in making FS-DFSP diagnosis as well as decrease/disappearance of CD34 immunoreactivity (18).

Furthermore, in light of GEP analysis results, immunohistochemical analysis was performed using antibodies against CD20 (clone L26; Dako; 1:400; antigen unmasking 96°C EDTA 15′) and CD57 (clone TB01; Dako; 1:100; antigen unmasking 96°C EDTA 30′). The sections were stained using a Dako Flex+ Autostainer (Dako). Three additional cases have been added to the series (cases 11, 12, and 13; Table 1) in order to interrogate FS-DFSP–naïve profile and to compare it with that of IM-treated cases.

FISH for detection of the *COL1A1–PDGFB* fusion gene

FISH analysis was performed in all the metastatic lesions. BACs clones (BACPAC Resource Center. C.H.O.R.I. Children's Hospital Oakland Research Institute Oakland, CA) for PDGFB (RP1-506F7 and RP11-630N12) and COL1A1 (RP11-93L18 and RP11-630N12) were labeled with Spectrum Orange and Spectrum Green (Vysis), respectively. FISH experiments were carried out accordingly to the manufacturer's instructions. At least 100 tumoral nuclei were scored for the presence of gene fusion.

Whole transcriptome sequencing

RNAseq analysis was performed on 6 cryopreserved FS-DFSP. We evaluated 4 naïve FS-DFSP samples, with tumor cellularity greater than 80% (patients 8, 11, 12,13,Table 1), and 2 post-IM FS-DFSP samples (in one case corresponding to patient 4 in Tables 1 and 2, the sample was obtained from a metastatic lesion resected in 2012; in the other case, the sample was taken from a locally relapsed tumor that appeared concomitantly to the metastatic lesions, corresponding to patient #2 in Tables 1 and 2). The hematoxylin and eosin (H&E) frozen control section of patient #4 showed a cellulate area made by 70% of viable tumor, whereas in H&E-frozen control section of patient #2, the residual viable tumor accounted for 30% of the specimen. Total RNA was extracted with the RNeasy Mini Kit (Qiagen), after mechanical dissociation with a pestle. cDNA libraries were synthesized from 250 ng of total RNA with the TruSeq RNA Sample Prep Kit v2 (Illumina) according to the manufacturer's instructions. Sequencing by synthesis was performed on HiScanSQ sequencer (Illumina) at 80 bp in paired-end mode. Approval of the present study by the Institutional Review Board was provided.

Gene expression profile analysis and variant detection

After demultiplexing and FASTQ generation (performed with BcltoFastq), the paired-end reads were mapped with the pipeline TopHat/Bowtie on human reference genome HG19, collected from UCSC Genome Browser (http://www.genome.ucsc.edu). After the alignment procedure, the BAM file obtained was processed with Samtools in order to remove the optical/PCR duplicate, and to perform the sorting and indexing procedures (19).

The detection of single-nucleotide variants (SNV) was performed with Mutect (20), while insertion and deletion (InDels) were called with GATK (21). The variations were filtered on dbSNP, 1000Genomes, and Exome Variant Server (EVS) in order to select the novel mutations that were then annotated with the software Annovar. SNVs and Indels were prioritized based on the predicted effect of genomic variant on protein structure and stability with a suite of computation tools, including Provean, SIFT, and Polyphen2.

The analysis of gene expression was performed in two steps: (i) the function htseq-count (Python package HTseq) was adopted to count the number of reads mapped on known genes, included in

Table 1. Pathology.

	Primary				Local recurrence			Metastasis					
Patient ID #	Diagnosis by year	Site	Morphology	IHC	Diagnosis by year	Morphology	IHC	Diagnosis by year	Site	Morphology	IHC	Imatinib treatment	Path response to imatinib
1	DFSP, 1987	Scalp	Usual	n.d.	1997	Unknown	Unknown	FS-DFSP, 2012 (biopsy; referred)	Lung, CNS	Spindle	$CD34^-$	No	—
2	DFSP, 1992	Trunk	Usual	n.d.	FS-DFSP (biopsy), 2013	Spindle	$CD34^+$	FS-DFSP, 2014 (tru-cut)	Lung, abdomen, soft tissue	Spindle	$CD34^+$	No	—
					FS-DFSP, 2013	Spindle	$CD34^+$						
3	DFSP, 2002	Groin	Usual	$CD34^+$	—	—	—	FS-DFSP, 2012	Lung (1 nodule, 3 cm)	Spindle	$CD34^+$	No	—
								FS-DFSP, 2014	Lung (1 nodule, 1.5 cm)	Spindle	$CD34^+$	Yes	0%
4	DFSP+ FS/DFSP, 2003 (referred)	Scalp	Spindle	$CD34^+$ DFSP; $CD34^-$ FS-DFSP	DFSP+ FS/DFSP, 2008	Spindle	$CD34^+$ DFSP; $CD34^-$ FS-DFSP	FS-DFSP, 2011	Lung (2 nodules, 1 and 1.2 cm)	Spindle	$CD34^-$	No	—
								FS-DFSP, 2012	Lung (3 nodules, 1.5, 1, 0.7 cm)	Spindle	$CD34^-$	Yes	30%, inflammatory components
								FS-DFSP, 2014	Lung (2 cm)	Spindle	$CD34^-$	Yes	70%, inflammatory components
5	DFSP+ FS/DFSP, 2001 (referred)	Trunk	Spindle	CD34 + focal	—	—	—	FS-DFSP, 2009 (referred)	STS, bone	Spindle	$CD34^-$	Yes	>50%
6	DFSP+ FS/DFSP, 2003 (referred)	Trunk	Myxoid	$CD34^+$ DFSP; $CD34^-$ FS-DFSP	—	—	—	FS-DFSP, 2006 (referred)	Lung	Myxoid	CD34 + focal	No	—
7	DFSP+ FS/DFSP, 2006 (referred)	Trunk	Spindle	$CD34^+$	—	—	—	FS-DFSP, 2007 (FNA; referred)	Lung	Spindle	$CD34^+$	No	—
								FS-DFSP, 2007	Lung (1 nodule, 8 cm)	Spindle	$CD34^+$	Yes	0%
8	DFSP+ FS/DFSP, 2008 (referred)	Scalp	Spindle	$CD34^+$	—	—	—	FS-DFSP, 2011 (treated)	Abdomen, STS	Spindle	$CD34^+$	No	—
								FS-DFSP, 2014	Abdomen, STS	spindle	$CD34^+$	Yes	60%
9	DFSP+ FS/DFSP, 2012 (referred)	Trunk	Spindle	$CD34^+$	—	—	—	FS-DFSP, 2014 (tru-cut; referred)	Pancreas	Spindle-pleomorphic	$CD34^+$ weak	No	—
10	DFSP+ FS/DFSP, 2008 (referred)	Scalp	Spindle	$CD34^+$	FS-DFSP (2010; referred)	Spindle	$CD34^+$	FS-DFSP (2014; tru-cut)	Pelvis	Spindle	$CD34^-$	Yes	0%
					FS-DFSP (2012; referred)	Spindle	$CD34^+$	FS-DFSP (2014; tru-cut)	Stomach	Spindle	$CD34^-$	Yes	0%
								FS-DFSP (2014; FNA)	Lung, pancreas, stomach, STS	Spindle	$CD34^-$	Yes	0%
11	DFSP+FS/DFSP, 2010	Groin	Myxoid	$CD34^+$	DFSP+FS/DFSP, 2012	Myxoid	$CD34^+$	FS-DFSP, 2012	Lung	Myxoid	$CD34^+$	—	—
12	DFSP+FS/DFSP, 2014	Thigh	Spindle	$CD34^+$	—	—	—	—	—	—	—	—	—
13	DFSP+FS/DFSP, 2014	Trunk	Spindle	$CD34^+$	—	—	—	—	—	—	—	—	—

Abbreviations: FNA, fine needle aspiration; IHC, immunohistochemistry; n.d., not determined.

Table 2. Patient characteristics

ID	Gender	Age at the time of first diagnosis/IM	Location of primary tumor	Disease extent at time of starting IM	Site of metastases at the time of starting IM	Treatment with IM	Best response (RECIST)	Best FDG-PET response	PFS (months)	Reason for IM definitive interruption	Surgery after IM	Response to IM at the time of surgery	Relapse after surgery	Relapse free from IM discontinuation and surgery (months)	Status at last FU
1	Male	35/61	Scalp	L, M	Lung, CNS	Yes	PD	Not assessed	2	Progression	NO	Not applicable	Not applicable	Not applicable	DOD
2	Male	48/70	Trunk	M	Lung, abdomen, soft tissue	Yes	PR	Not assessed	7	Progression	NO	Not applicable	Not applicable	Not applicable	AWD
3	Male	37/50	Groin	M	Lung	Yes	PR	PR	10+	Ongoing	Yes	Yes	Yes	6	AWD
4	F	50/59	Scalp	M	Lung	Yes	PR	PR	25	Progression	Yes	Yes	Yes	12	AWD
5	F	45/55	Trunk	M	Soft tissue, bone	Yes	PR	Not assessed	11	Progression	Yes	Yes	Yes	5	DOD
6	Male	69/73	Trunk	M	Lung	Yes	PR	PR	9	Progression	No	Not applicable	Not applicable	Not applicable	DOD
7	Male	46/49	Trunk	M	Lung	Yes	PR	PR	4	Progression	Yes	No progression	Yes	5	DOD
8	Male	48/53	Scalp	M	Abdomen, soft tissue	Yes	PR	PR	22	Progression	Yes	Yes	Yes	5	AWD
9	Male	41/53	Trunk	M	Abdomen (pancreas)	Yes	PR	Not assessed	5	Toxicity	No	Not applicable	Not applicable	Not applicable	AWD
10	F	43/50	Scalp	L, M	Lung, abdomen (pancreas, stomach), soft tissue	Yes	SD	Not assessed	3+	Ongoing	No	Not applicable	Not applicable	Not applicable	AWD

Abbreviations: AWD, alive with disease; CNS, central nervous system; DOD, dead of disease; F, female; FU, follow up; IM, imatinib; L, local; M, metastatic; PFS, progression free survival.

the Ensembl release 72 annotation features (http://www.ensembl.org); (ii) the differential expressed genes were modeled with the negative binomial distribution using the R-Bioconductor package edgeR. Hierarchical clustering of differentially expressed genes and unsupervised Principal Component Analysis were performed with Multiple Array Viewer (MEV available at http://www.tm4.org/mev.html). Pathway analysis was performed on the KEGG database with David/EASE tool (http://david.abcc.ncifcrf.gov).

Medical therapy and efficacy assessment

Patients included in this study had to have a metastatic DFSP/FS-DFSP, a performance status (ECOG) $\leq$3, an adequate bone marrow, and organ function in order to receive IM. All Patients gave their written informed consent to the treatment.

Patients received oral IM 400 mg, OD, continuously till progression or planned surgical resection. In case of resistance, the daily dose of IM was tentatively increased to 800 mg/day. At baseline, all patients were evaluated with medical history and physical examination, a complete blood count and serum chemistry and cardiologic assessment. A whole-body CT scan and a CT or MRI of the sites of disease were also required. PET scan was performed in some cases. Tumor assessment was performed after 8 to 12 weeks from starting treatment, then every 2 months, in case of suspected progression and before surgery.

Response was assessed according to RECIST (version 1.1; ref. 22). PET response was evaluated according to the European Organization for Research and Treatment of Cancer (EORTC) 1999 criteria (23). Overall survival (OS) and progression-free survival (PFS) were estimated by the Kaplan–Meier method. All patients receiving at least one dose of IM were included in the analysis. Patients were censored at the last contact. Death of any cause was considered therapy failure. To estimate the PFS, patients progressing after IM discontinuation whose response was restored after restarting IM were considered progressing at the time of definitive progression on IM.

Results

Clinical findings

Out of 52 patients who requested a treatment with IM for a DFSP or an FS-DFSP from January 2007 to March 2015, 10 cases with metastatic disease were identified. Three cases had been initially operated for their primary tumor in our institution, while 7 presented to our attention at the time of relapse.

Median age at the time of treatment with IM was 53 years (range, 49–73); female/male ratio was 3/7. The ECOG performance status was $\leq$2 in 7 cases, 3 in 3. All patients had been pretreated with surgery. Three patients were treated with radiotherapy, 2 with chemotherapy, and 1 with IM (in the local phase of the disease). Site of metastases at the time of treatment with IM were lung (7), abdomen (4), soft tissue (4), bone (1), and brain (1; Table 2).

All patients were evaluated by CT scan.

All patients started IM 400 mg/day. In 4 cases, IM was increased to 800 mg, twice a day, after the evidence of progression (one primary resistance, 3 secondary resistance); in 2 patients, dose escalation was not feasible due to patient's comorbidities. IM was continued until evidence of progression or complete surgical resection of the residual tumor or toxicity. Overall, IM was well tolerated. Temporary treatment interruptions due to G2-3

neutropenia and G2 fluid retention were necessary in 3 cases; in one case, IM was definitively stopped due to toxicity (G2 anorexia and G3 anemia followed by worsening of general condition).

Efficacy assessment

All cases are evaluable for response. At the time of the present analysis, 2 patients are still on therapy, 7 stopped treatment for progression while under therapy and one for toxicity.

Best RECIST response was: 8 partial response (PR; 70%), 1 stable disease (SD), 1 progressive disease (PD). All responses were confirmed at 3 months. PET response was consistent with PR RECIST in the 5 cases that were evaluated. In the single patient (case 1, Table 2) who progressed soon after starting IM, the drug was increased to 800 mg, again with PD. This patient died in 5 months. In 3 further cases who progressed after the evidence of an initial response, IM was increased to 800 mg/day, with PD (cases 2, 5, and 7). Five patients received complete surgical excision of the residual tumor after IM, after 5, 4, 5, 9, and 5 months from starting IM, respectively. Four cases were operated at INT, the fifth patient required a neurosurgical procedure performed in another hospital. Four of them were resected while under response; the disease was located to the lung in 3 cases, and to the bone in one; in all cases, preoperative CT scan showed a single metastatic lesion, but in one of them, three nodules were discovered at the time of the surgical procedure. The fifth patient received surgery after PD. A pathologic response was evident in 3 patients (see "Pathology" paragraph), with aspects depending on surgical timing and affecting tumor cells and stroma. All the 4 patients who were operated while under response to IM relapsed, after 12, 6, 5, and 5 months, respectively. IM was restored in 4 patients with a new response. Three of those cases eventually progressed after 4 months from IM re-start, while one is still on treatment. Median PFS was 11 months (range, 2–25). Median OS has not yet been reached.

Pathology

Pathologic features of patients treated with IM are detailed in Table 1 (patients 1–10). All patients had histologic confirmation of their distant relapse. In all cases, the pathologic appearance was consistent with an FS-DFSP. The primary tumor showed classic DFSP aspects without an FS component in 3 patients, who had the longest relapse-free survival (25, 22, and 10 years). In 6 cases, the primary tumor retained focal marginal areas of classic/low-grade DFSP together with FS areas featuring spindle cells; one case showed myxoid aspects. The concomitance of a low- and high-grade component was also showed by 1 local recurrences, whereas the metastatic lesions exhibited only FS features; in addition, in one case, extensive necrotic areas were detected. No morphologic changes in the pattern of growth were observed in 9 of 10 cases comparing primary tumor, recurrence, and metastasis, whereas one case (assessed by tru-cut) exhibited additional pleomorphic area in the metastatic tissue. In 2 of 8 cases, CD34 immune-positivity was lost in the high-grade component of the primary tumor.

After IM treatment, tumor samples were available in 5 cases. They exhibited different aspects depending on surgical timing, with changes in tumor cellularity that—from baseline—ranged from 0% to 70%. More frequently, there were cellular-depleted areas replaced by hyalinized stroma (Supplementary Fig. S1). In other cases, we detected changes consistent with early signs of response to IM, marked by a variable inflammatory component and intermingled with scattered viable tumor cells (Supplementary Fig. S1, corresponding to patient 4, Tables 1 and 2, whose matched cryopreserved halve was used for RNAseq analysis). The presence of immune/inflammatory infiltrate is in line with the GEP analysis results described below. Immunohistochemistry failed to highlight decrease of PDGFRB expression in the viable tumor cells surrounding the regressed areas (data not shown). This is consistent with our previous reports on the lack of evidence of PDGFRB decrease/switch-off in IM-responsive DFSP patients, as assessed by both IHC and immunoblot (5).

Whole transcriptome sequencing

To gain insight into the biologic activity exerted by IM in FS-DFSP, RNAseq transcriptional profile was performed on 6 FS-DFSP for which frozen material was available, including 4 naïve cases (2 localized and 2 metastatic) and 2 post-IM treatment samples. All cases retained the *COL1A1–PDGFB* fusion.

Naïve and IM-treated samples clustered separately by unsupervised Principal Component Analysis, indicating a significantly different GEP analysis (Fig. 1A). Supervised analysis highlighted the differential expression of 250 genes, with a P value <0.01 and 2-fold difference (Supplementary Table S1; Fig. 1B).

IM-treated samples displayed an enhanced expression of genes involved in drug and xenobiotics metabolism, a finding not completely unexpected, and a significant downregulation of components of kinase signaling pathways, such as TGFB2, PDGFD, and TGFBR1 (Fig. 1B and C; Table 3). The expression of *PDGFB* and *COL1A1* was observed both in untreated and treated samples.

Seven of the top overexpressed genes displaying a Log2 ratio equal or higher than 3.5 in IM-treated samples were related to the innate or adaptive immune system. These 7 genes included genes related to B-cell responses and encoding for constant and variable chains of the immunoglobulin family together with genes associated with natural killer (NK)–mediated functions, with internal T-cell signaling (24), and with myeloid cells differentiation (ref. 25; Table 4). IHC analysis performed in post-IM samples (Table 1, patient 4) using anti-CD20 and CD57-specific antibodies confirmed the presence of tumor-infiltrating lymphoid cells expressing B- and NK-specific markers (Fig. 2). Six genes related to endothelial cells and angiogenesis also belonged to this top list. These genes encoded for proteins regulating at different levels the endothelial/vascular permeability (26–28) and differentiation of endothelial cells (29) and included both transcription factors and adhesion molecules. Moreover, VEGF-related genes, such as the gene encoding for VEGFR3 or enzyme affecting HIF1 and VEGF expression, resulted also upregulated in IM-treated tumors (Table 4; ref. 30).

Pathway enrichment analysis confirmed the modulation of genes related to the immune response, with genes involved in antigen processing and presentation and in NK-mediated cytotoxicity being overrepresented in IM-treated samples (Table 3; Fig. 1C).

Discussion

In this series of 10 histologically confirmed, metastatic DFSP patients treated with IM, we found that all lesions were made up of FS-DFSP, and, as expected, retained the *COL1A1–PDGFB* rearrangement. The RECIST response rate was 80%, with only 1 patient showing a primary resistance. Neither primary nor

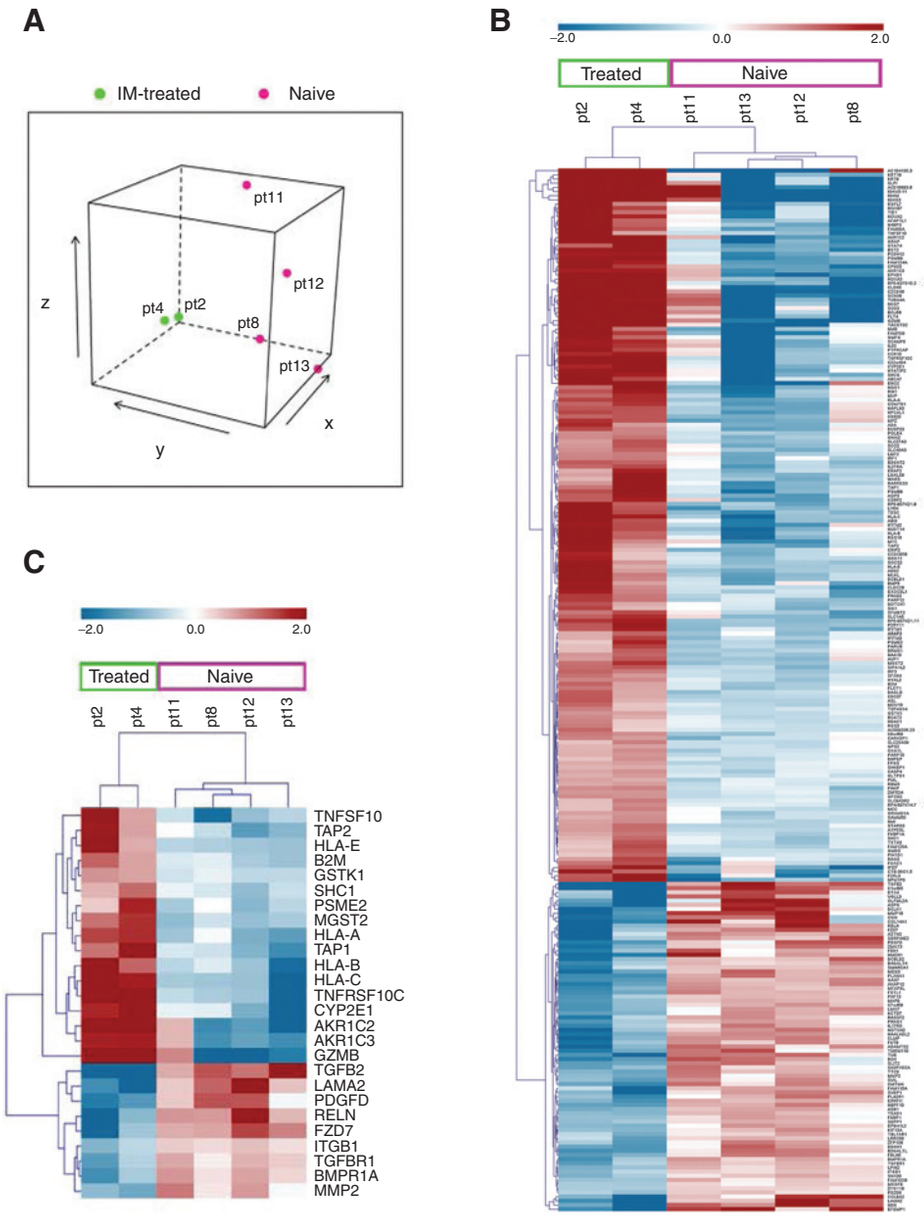

Figure 1.
A, naïve and IM-treated samples clustered separately by unsupervised Principal Component Analysis, indicating a significantly different GEP analysis. B, supervised hierarchical cluster of differentially expressed genes between naïve and IM-treated samples. C, hierarchical cluster of the genes highlighted in the pathway enrichment analysis.

secondary resistance could be overcome by increasing the dose of IM to 800 mg/day. Median PFS was only 11 months. All 5 patients undergoing a complete surgical resection after IM relapsed afterwards. IM was restored in the 4 patients with no previous evidence of resistance to IM, obtaining a new transient response. Contrary to naïve FS-DFSP, RNAseq analysis of IM-treated patients revealed a strong modulation of genes involved in drug/xenobiotic metabolism and those regulating tumor-related kinase signaling. Immune-related genes were also affected by IM.

Although retrospective and limited to 10 cases, this is the largest series of metastatic DFSP patients treated with IM. In fact, metastatic relapse is an extraordinary rare event in DFSP/FS-DFSP. We confirm that IM is active in the vast majority of patients who develop metastases from DFSP/FS-DFSP. However, primary resistance is observed and median PFS is shorter than reported in series including nonmetastatic DFSP. The first two reports on IM activity in DFSP were by Rubin and colleagues (10) and by Maki and colleagues (12) in 2002 in 3 DFSP metastatic patients, with evidence of a major response in 2 cases, whereas the third patient had a transient response and eventually underwent a rapid progression (12). IM activity was further confirmed within 6 prospective phase II studies (11, 13–15, 31). The largest was reported in 2010 (31) on 25 patients treated with neoadjuvant IM, but included only localized, classic DFSP. The second largest series was obtained pulling together the phase II studies run by EORTC and SWOG (11). The analysis showed a 46% response rate by RECIST (e.g., 11 PR of 21 evaluable patients) and a 1.7-month median time to progression. Interestingly, the activity of IM was not superimposable in classic DFSP and FS-DFSP: all 11 patients carrying a classic DFSP benefited from IM, whereas 2 of 8

Table 3. Pathway enrichment analysis of upregulated (A) and downregulated genes (B) in the IM-treated samples with respect to naïve samples

KEGG_Pathway	*P*	Genes	Fold enrichment
A. Upregulated genes			
Antigen processing and presentation	0.00029	*PSME2, TAP2, TAP1, HLA-A, HLA-C, HLA-B, HLA-E, B2M*	7.39
NK-cell–mediated cytotoxicity	0.0034	*TNFSF10, TNFRSF10C, HLA-A, GZMB, HLA-C, SHC1, HLA-B, HLA-E*	4.61
Metabolism of xenobiotics by cytochrome P450	0.0043	*AKR1C3, AKR1C2, GSTK1, CYP2E1, MGST2*	7.31
Allograft rejection	0.0073	*HLA-A, GZMB, HLA-C, HLA-B, HLA-E*	9.74
Graft-versus-host disease	0.0092	*HLA-A, GZMB, HLA-C, HLA-B, HLA-E*	8.99
Type I diabetes mellitus	0.011	*HLA-A, GZMB, HLA-C, HLA-B, HLA-E*	8.35
Autoimmune thyroid disease	0.019	*HLA-A, GZMB, HLA-C, HLA-B, HLA-E*	6.88
B. Downregulated genes			
Pathways in cancer	0.0059	*LAMA2, TGFBR1, ITGB1, MMP2, FZD7, TGFB2*	4.65
Focal adhesion	0.037	*LAMA2, RELN, PDGFD, ITGB1*	5.06
Colorectal cancer	0.038	*TGFBR1, FZD7, TGFB2*	9.08
ECM–receptor interaction	0.038	*LAMA2, RELN, ITGB1*	9.08
TGF-beta signaling pathway	0.041	*TGFBR1, BMPR1A, TGFB2*	8.77

FS-DFSP had a progression as their best response. In addition, primary or secondary resistance was observed in 6 of 7 patients with metastatic disease. Overall, DSFP metastatic cases included in several case reports or case series (7) is less sensitive to IM.

Interestingly, all our metastatic cases were found to have a FS component in the metastatic tissue. Seven were FS from the onset of disease. In 3 cases, the review of primary samples did not show FS aspects. Thus, one cannot exclude that FS areas were already present in other areas of the primary lesions. Interestingly, however, these patients without an apparent FS component at onset had the longest previous relapse-free survival (25, 22, and 10 years). Thus, retrospective studies on surgical series with an updated pathologic review are needed to clarify to which extent classic DFSP, i.e., those without any FS aspect, do have a metastatic potential.

In this series, all patients who were operated after being treated with IM had a relapse, suggesting that IM is incapable of eradicating metastatic DFSP/FS-DFSP and the role of surgery is limited. It follows that policies of re-establishment of IM after surgery of responding metastatic disease should be pursued in DFSP. This is standard practice in metastatic gastrointestinal stromal tumor (GIST) surgically excised of IM-responding lesions (32).

To gain insights into the mechanism of action of IM in FS-DFSP, we compared the transcriptional profile of naïve versus IM-treated samples. GEP analysis confirmed that the post-IM samples obtained from patients with radiologic and pathologic evidence of response maintained the expression of DFSP-associated transcripts *COL1A1* and *PDGFB*. Moreover, GEP analysis underscored significant changes in the transcriptional profile of IM-treated samples, which displayed a molecular signature indicative of a modulation of innate and adaptive immunity, changes in vascular permeability, and silencing of some kinase signaling pathways that mainly involve TGFb. Among genes upregulated in IM-treated samples, we found those encoding constant and variable chains of the immunoglobulin family and genes encoding components of the NK pathway and NK-mediated lysis, such as NKG7 and GZMB. These findings correlated with the pathologic evidence in these specimens of B cells, which likely play a role in adaptive-specific immunity and in Fc receptor–dependent phagocytosis, and CD57-positive lymphoid cells, essentially consisting of finally differentiated, cytotoxic-competent NK cells (33, 34). This strongly suggests that IM-induced alterations on tumor cells in turn trigger the activation of this innate response in DFSP/FS-DFSP, as already described in GIST (35–37). Genes belonging to antigen processing and presentation were also overrepresented in posttreatment samples. This is suggestive of modulation also of the adaptive immune cell response and supports the hypothesis of an enhanced susceptibility of IM-treated tumor cells to an antigen-specific, HLA-restricted immune recognition. A direct comparison of matched pre- and post-IM samples will eventually allow to draw definitive conclusions on the contribution of modulation of the innate and, likely, adaptive immune response in the efficacy of IM treatment in DFSP/FS-DFSP. Functional immunological

Table 4. List of immune- and vascular-related genes upregulated in IM-treated tumors and displaying FC equal or higher than 3.5 log2 ratio (log2R).

Gene	Log2R	*P*	Description
IGHG3	9.7	0.00089	Heavy constant gamma chain 3, Immunoglobuline, B-cell response
IGHM	7.1	0.00678	Heavy constant mu chain, Immunoglobuline—B cells response
IGKV3-11	6.4	0.00731	Kappa variable 3-11 chain, Immunoglobulin, B cells
GZMB	4.7	0.00396	Granzyme B, NK, and cytotoxic T-lymphocyte–associated serine esterase 1
NKG7	4.0	0.00612	NK cell granule protein 7
GRAP	3.9	0.00011	GRB2-related adaptor protein. Molecule involved in TGFB and CD28 signaling (15, 16)
SLPI	6.4	0.00754	Secretory leukocyte peptidase inhibitor. Involved in the differentiation of myeloid cells (16)
CLDN5	5.5	0.00070	Claudin 5, Claudins are integral membrane proteins and components of tight junction strands (17, 18)
C2CD4B, (alias NLF2)	5.5	0.00856	C2 calcium-dependent domain containing 4B, expressed by endothelial cells and regulating vascular permeability. Involved in regulating genes controlling cellular architecture (19)
HOXA3	3.5	0.00927	HOXA3 transcription factor. Accelerates wound repair by mobilizing endothelial progenitor cells and by attenuating the excessive inflammatory response of chronic wounds (20)
FLT4	4.0	0.00106	Fms-related tyrosine 4, receptor for VEGFRC, known also as VEGFR3
SOD3	3.9	0.00532	Superoxide dismutase 3. SODs are antioxidant enzymes that catalyze the dismutation of two superoxide radicals into hydrogen peroxide and oxygen. Involved in the negative regulation of HIF1 and VEGFR expression (21)

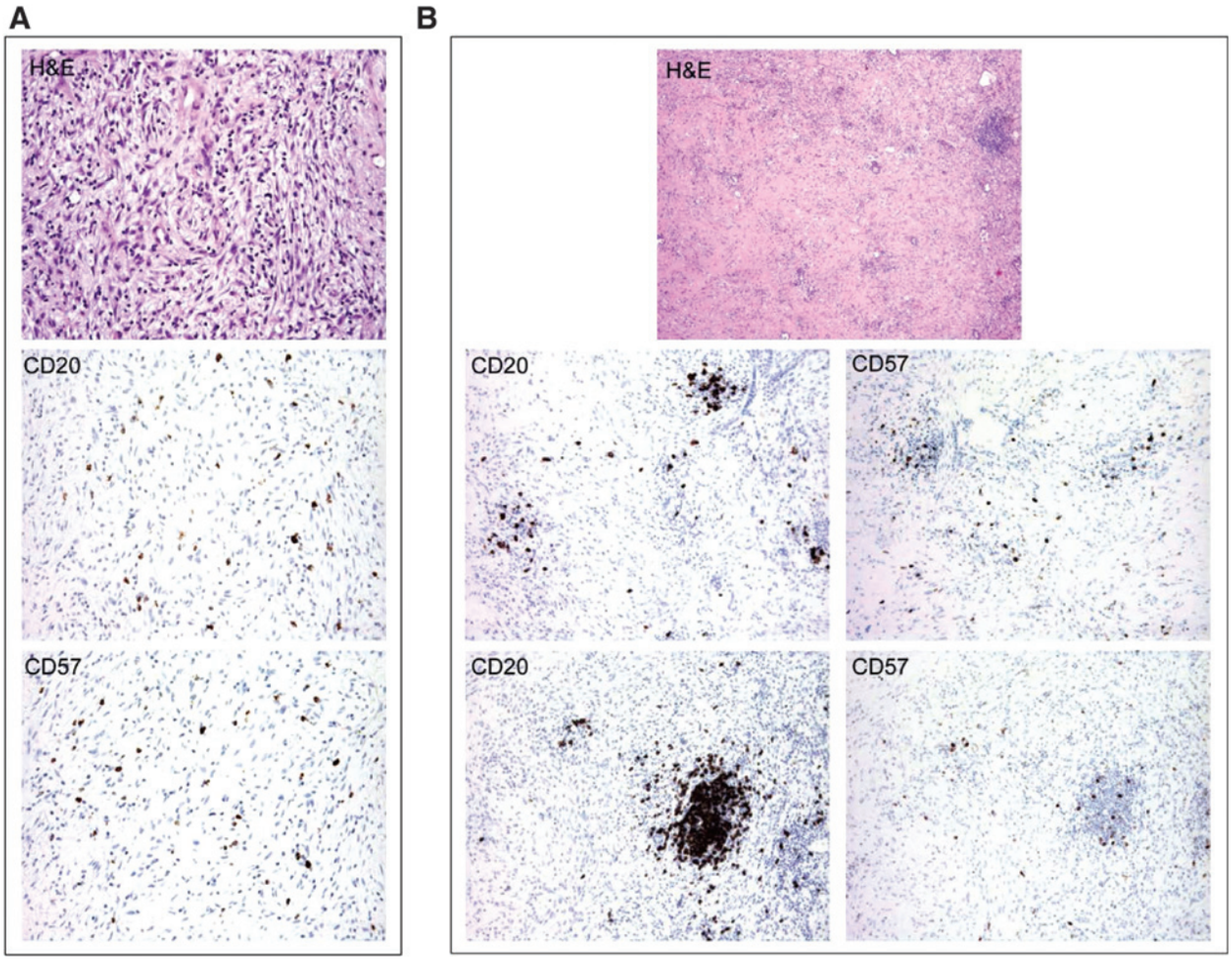

Figure 2.
B- and NK-cell infiltration in a metastatic FS-DFSP lesion after treatment with IM, corresponding to patient #4 in Tables 1 and 2. H&E, CD20 (B cells), and CD57 (NK cells) stains are shown. A, the metastatic tumor after the first period of treatment with IM, followed by surgery in 2012 (this is the sample evaluated also by RNA-seq). B, the relapsed tumor retreated with IM, and again resected in 2014. B- and NK-cell infiltration was already evident in the first post-IM lesions (A) and even more pronounced in the second one (B). A, original magnification, ×100; B, original magnification, ×20 (H&E) and ×50 (CD20 and CD57 stainings).

studies on both T-cell and NK-mediated immunity are currently ongoing, taking advantage of few fresh cryopreserved cellular suspensions of post-IM tumor samples. Moreover, the role of TGFb signaling and the presence of nonsynonymous mutations possibly involved in response to IM are under evaluation.

We could observe 1 patient with primary resistance to IM and 5 cases with progression after response. The basis for the resistance to IM in DFSP/FS-DFSP is still a matter of discussion and does not seem to be related to PDGFRB (5). Unfortunately, the lack of samples suitable to RNAseq analyses prevented us from fully exploring the mechanisms underlying resistance. By whole-genomic sequencing, Hong and colleagues examined one case of DFSP prior and after development of resistance to IM, and identified 8 nonsynonymous somatic gene mutations, involving ACAP2, CARD10, KIAA0556, PAAQR7, PPP1R39, SAFB2, STARD9, and ZFYVE9, in the IM-resistant tumor tissue (16). This study revealed diverse possible candidate mechanisms by which IM resistance to PDGFRB inhibition may arise in DFSP. We failed to detect somatic or deleterious mutations in our RNAseq, although variant calling from RNAseq data is notoriously less efficient compared with genome/exome analyses.

Eilers and coworkers demonstrated CDKN2A deletion in a subset of FS-DFSP, providing evidence of a contribution of p16 loss to DFSP progression (9). Neither study highlighted a role for PDGFRB genetic alteration in IM resistance. Rather, results by Eilers and colleagues seem to support a role for candidates downstream of PDGFRB. Linn and colleagues (38) reported that DFSP expresses high levels of GRB2 and PRKA, both downstream to the PDGF receptor. Intriguingly, our gene expression analysis showed an upregulation of the GRAP gene, encoding the GRB2-related adaptor protein, responsible for the coupling of signals from receptor and cytoplasmic tyrosine kinases to the Ras signaling pathway. On this basis, it is tempting to speculate that this adaptor has a role in DFSP progression (39).

In conclusion, our study confirms that IM is active in the majority of metastatic DFSP, but duration of response is inferior than in published series which included both DFSP and FS-DFSP. In our series, all metastatic patients had an FS-DFSP. We failed to

eradicate the tumor even in those patients responsive to IM who could undergo a complete surgical resection, suggesting that the role of surgery is limited. IM reintroduction should be considered on relapse. Finally, IM treatment was found to have an impact also on tumor microenvironment, in terms of increased permeability of endothelial cells and immune infiltrates. This suggests that the elicitation of an innate and adaptive immune response may be crucial in sustaining DFSP-FS response to the treatment.

Disclosure of Potential Conflicts of Interest

S. Stacchiotti reports receiving a commercial research grant from Novartis. M. A. Pantaleo reports receiving a commercial research grant from Novartis and speakers bureau honoraria from Pfizer. A. Gronchi and P.G. Casali report receiving speakers bureau honoraria from and are consultant/advisory board members for Novartis. M. Fiore reports receiving speakers bureau honoraria from Novartis. No potential conflicts of interest were disclosed by the other authors.

Authors' Contributions

Conception and design: S. Stacchiotti, A.P. Dei Tos, F. Grosso, C. Castelli, P.G. Casali

Development of methodology: S. Stacchiotti, M.A. Pantaleo, A. Astolfi, G.P. Dagrada, M. Urbini, F. Grosso, S. Pilotti, P.G. Casali

Acquisition of data (provided animals, acquired and managed patients, provided facilities, etc.): S. Stacchiotti, M.A. Pantaleo, A. Astolfi, M. Urbini, A. Gronchi, M. Fiore, E. Conca, E. Palassini, B. Vincenzi, F. Grosso

Analysis and interpretation of data (e.g., statistical analysis, biostatistics, computational analysis): S. Stacchiotti, M.A. Pantaleo, T. Negri, M. Tazzari, G.P. Dagrada, R. Maestro, A. Gronchi, A.P. Dei Tos, C. Castelli, P.G. Casali

Writing, review, and/or revision of the manuscript: S. Stacchiotti, T. Negri, M. Tazzari, R. Maestro, A. Gronchi, M. Fiore, E. Conca, B. Vincenzi, F. Grosso, S. Pilotti, C. Castelli, P.G. Casali

Administrative, technical, or material support (i.e., reporting or organizing data, constructing databases): S. Stacchiotti, A. Gronchi

Study supervision: S. Stacchiotti, A. Gronchi, A.P. Dei Tos, B. Vincenzi, C. Castelli, P.G. Casali

Grant Support

This study was funded by Associazione Italiana per la Ricerca sul Cancro (AIRC; MFAG 11817 to T. Negri) and by Fondazione Italiana Ricerca sul Cancro (FIRC) with a fellowship for M. Tazzari.

The costs of publication of this article were defrayed in part by the payment of page charges. This article must therefore be hereby marked *advertisement* in accordance with 18 U.S.C. Section 1734 solely to indicate this fact.

Received May 27, 2015; accepted July 27, 2015; published OnlineFirst August 10, 2015.

References

1. Fletcher CDM, et al. World Health Organization (WHO) classification of tumours of soft tissue and bone. Pathology and Genetics. Lyon: IARC Press; 2013. p. 80–82.
2. Simon MP, Pedeutour F, Sirvent N, Grosgeorge J, Minoletti F, Coindre JM, et al.: Deregulation of the platelet-derived growth factor B-chain gene via fusion with collagen gene COL1A1 in dermatofibrosarcoma protuberans and giant-cell fibroblastoma. Nat Genet 1997;15:95–98.
3. Greco A, Fusetti L, Villa R, Sozzi G, Minoletti F, Mauri P, et al. Transforming activity of the chimeric sequence formed by the fusion of collagen gene COL1A1 and the platelet derived growth factor b-chain gene in dermatofibrosarcoma protuberans. Oncogene 1998;17:1313–9.
4. Fiore M, Miceli R, Mussi C, Lo Vullo S, Mariani L, Lozza L, et al. Dermatofibrosarcoma protuberans treated at a single institution: a surgical disease with a high cure rate. J Clin Oncol 2005;23:7669–75.
5. Stacchiotti S, Pedeutour F, Negri T, Conca E, Marrari A, Palassini E, et al. Dermatofibrosarcoma protuberans-derived fibrosarcoma: clinical history, biological profile and sensitivity to imatinib. Int J Cancer 2011;129: 1761–72.
6. Abbott JJ, Oliveira AM, Nascimento A. The prognostic significante of fibrosarcomatous transformation in dermatofibrosarcoma protuberans. Am J Surg Pathol 2006;30:436–443.
7. Dhir M, Crockett DG, Stevens TM, Silberstein PT, Hunter WJ, Foster JM. Neoadjuvant treatment of Dermatofibrosarcoma protuberans of pancreas with Imatinib: case report and systematic review of literature. Clin Sarcoma Res 2014;4:8.
8. Stiller CA, Trama A, Serraino D, Rossi S, Navarro C, Chirlaque MD, et al. Descriptive epidemiology of sarcomas in Europe: report from the RARECARE project. Eur J Cancer 2013;49:684–95.
9. Eilers G, Czaplinski JT, Mayeda M, Bahri N, Tao D, Zhu M, et al. CDKN2A/p16 loss implicates CDK4 as a therapeutic target in imatinib-resistant dermatofibrosarcoma protuberans. Mol Cancer Ther 2015;14:1346–53.
10. Rubin BP, Schuetze SM, Eary JF, Norwood TH, Mirza S, Conrad EU, et al. Molecular targeting of platelet-derived growth factor B by imatinib mesylate in a patient with metastatic dermatofibrosarcoma protuberans. J Clin Oncol 2002;20:3586–91.
11. Rutkowski P, Van Glabbeke M, Rankin CJ, Ruka W, Rubin BP, Debiec-Rychter M, et al. Imatinib mesylate in advanced dermatofibrosarcoma protuberans: pooled analysis of two phase II clinical trials. J Clin Oncol 2010;28:1772–9.
12. Maki RG, Awan RA, Dixon RH, Jhanwar S, Antonescu CR. Differential sensitivity to imatinib of 2 patients with metastatic sarcoma arising from dermatofibrosarcoma protuberans. Int J Cancer 2002;100:623–6.
13. Kérob D, Porcher R, Vérola O, Dalle S, Maubec E, Aubin F, et al. Imatinib mesylate as a pre-operative therapy in dermatofibrosarcoma: results of a multicentric phase II study on 25 patients. Clin Cancer Res 2010;16: 3288–95.
14. McArthur GA, Demetri GD, van Oosterom A, Heinrich MC, Debiec-Rychter M, Corless CL, et al. Molecular and clinical analysis of locally advanced dermatofibrosarcoma protuberans treated with imatinib: Imatinib Target Exploration Consortium Study B2225. J Clin Oncol 2005;23:866–73.
15. Sugiura H, Fujiwara Y, Ando M, Kawai A, Ogose A, Ozaki T, et al. Multicenter phase II trial assessing effectiveness of imatinib mesylate on relapsed or refractory KIT-positive or PDGFR-positive sarcoma. J Orthop Sci 2010;15:654–60.
16. Hong JY, Liu X, Mao M, Li M, Choi DI, Kang SW, et al. Genetic aberrations in imatinib-resistant dermatofibrosarcoma protuberans revealed by whole genome sequencing. PLoS One 2013;8:e69752.
17. Goldblum JR, Folpe AL, Weiss SW. Soft tissue tumors. 6th ed. Enzinger and Weiss; 2014, chapter 12, 387–400.
18. Hornick JL. Practical soft tissue pathology. A diagnostic approach. Elsevier Saunders; 2013. p. 399–403.
19. Pantaleo MA, Astolfi A, Indio V, Moore R, Thiessen N, Heinrich MC, et al. SDHA loss-of-function mutations in KIT-PDGFRA wild-type gastrointestinal stromal tumors identified by massively parallel sequencing. J Natl Cancer Inst 2011;103:983–7.
20. Cibulskis K, Lawrence MS, Carter SL, Sivachenko A, Jaffe D, Sougnez C, et al. Sensitive detection of somatic point mutations in impure and heterogeneous cancer samples. Nat Biotechnology 2013;31:213–9.
21. McKenna A, Hanna M, Banks E, Sivachenko A, Cibulskis K, Kernytsky A, et al. The Genome Analysis Toolkit: a MapReduce framework for analyzing next-generation DNA sequencing data. Genome Res 2010;20: 1297–303.
22. Eisenhauer EA, Therasse P, Bogaertsc J, Schwartz LH, Sargent D, Ford R, et al. New response evaluation criteria in solid tumours: Revised RECIST guideline (version 1.1). Eur J Cancer 2009;45:228–247.
23. Young H, Baum R, Cremerius U, Herholz K, Hoekstra O, Lammertsma AA, et al. Measurement of clinical and subclinical tumour response using [18F]-fluorodeoxyglucose and positron emission tomography: review and 1999 EORTC recommendations. European Organization for Research and Treatment of Cancer (EORTC) PET Study Group. Eur J Cancer 1999;35: 1773–82.
24. Schneider H, Rudd CE. CD28 and Grb-2, relative to Gads or Grap, preferentially co-operate with Vav1 in the activation of NFAT/AP-1 transcription. Biochem Biophys Res Commun 2008;369:616–21.

25. Klimenkova O, Ellerbeck W, Klimiankou M, Ünalan M, Kandabarau S, Gigina A, et al. A lack of secretory leukocyte protease inhibitor (SLPI) causes defects in granulocytic differentiation Blood 2014;123:1239–49.
26. Armstrong SM, Wang C, Tigdi J, Si X, Dumpit C, Charles S, et al. Influenza infects lung microvascular endothelium leading to microvascular leak: role of apoptosis and claudin-5. PLoS One 2012;7:e47323.
27. Kluger MS, Clark PR, Tellides G, Gerke V, Pober JS. Claudin-5 controls intercellular barriers of human dermal microvascular but not human umbilical vein endothelial cells. Arterioscler Thromb Vasc Biol 2013;33: 489–500.
28. Warton K, Foster NC, Gold WA, Stanley KK. A novel gene family induced by acute inflammation in endothelial cells. l. Gene 2004;342:85–95.
29. Kuo JH, Cuevas I, Chen A, Dunn A, Kuri M, Boudreau N. Secreted HoxA3 promotes epidermal proliferation and angiogenesis in genetically modified three-dimensional composite skin constructs. Adv Wound Care (New Rochelle) 2014;3:605–13
30. Sibenaller ZA, Welsh JL, Du C, Witmer JR, Schrock HE, Du J, et al. Extracellular superoxide dismutase suppresses hypoxia-inducible factor-1α in pancreatic cancer. Free Radic Biol Med 2014;69:357–66.
31. Ugurel S, Mentzel T, Utikal J, Helmbold P, Mohr P, Pföhler C, et al. Neoadjuvant imatinib in advanced primary or locally recurrent dermatofibrosarcoma protuberans: a multicenter phase II DeCOG trial with long-term follow-up. Clin Cancer Res 2014;20:499–510.
32. ESMO/European Sarcoma Network Working Group. Gastrointestinal stromal tumours: ESMO Clinical Practice Guidelines for diagnosis, treatment and follow-up. Ann Oncol 2014;25:iii21–6.
33. Lopez-Vergès S, Milush JM, Pandey S, York VA, Arakawa-Hoyt J, Pircher H, et al. D57 defines a functionally distinct population of mature NK cells in the human CD56dimCD16+ NK-cell subset. Blood 2010;116: 3865–74.
34. Montaldo E, Del Zotto G, Della Chiesa M, Mingari MC, Moretta A, De Maria A, et al. Human NK cell receptors/markers: a tool to analyze NK cell development, subsets and function. Cytometry A 2013;83: 702–13.
35. Ménard C, Blay JY, Borg C, Michiels S, Ghiringhelli F, Robert C, et al. Natural killer cell IFN-gamma levels predict long-term survival with imatinib mesylate therapy in gastrointestinal stromal tumor-bearing patients. Cancer Res 2009;69:3563–9.
36. Rusakiewicz S, Semeraro M, Sarabi M, Desbois M, Locher C, Mendez R, et al. Immune infiltrates are prognostic factors in localized gastrointestinal stromal tumors. Cancer Res 2013;73:3499–510.
37. Borg C, Terme M, Taïeb J, Ménard C, Flament C, Robert C, et al. Novel mode of action of c-kit tyrosine kinase inhibitors leading to NK cell-dependent antitumor effects. J Clin Invest 2004;114:379–88.
38. Linn SC, West RB, Pollack JR, Zhu S, Hernandez-Boussard T, Nielsen TO, Rubin BP, et al. Gene expression patterns and gene copy number changes in dermatofibrosarcoma protuberans. Am L Path 2003;163: 2383–95.
39. Cummins TD, Barati MT, Coventry SC, Salyer SA, Klein JB, Powell DW. Quantitative mass spectrometry of diabetic kidney tubules identifies GRAP as a novel regulator of TGF-beta signaling. Biochim Biophys Acta 2010;1804:653–61.